

## On the Mass Impact Loading of Ductile Plates\*

Norman Jones

University of Liverpool, Liverpool L69 3GH, UK

### ABSTRACT

This paper examines the response of circular and square plates struck by a rigid mass at the plate centre with a sufficient initial kinetic energy to produce large inelastic deformations. A simplified analysis, which retains finite-deflection effects and assumes that the plates are made of a rigid, perfectly plastic material, provides a relatively simple theoretical solution for the maximum permanent transverse displacement and the response duration. It transpires that the theoretical predictions give reasonable agreement with the maximum permanent transverse displacements recorded in several experimental studies on fully clamped, circular and square ductile metal plates. The final theoretical expressions for the behaviour are easy to use and ideal for preliminary design purposes and would be sufficiently accurate for final designs in some applications.

**Keywords:** Impact, square plate, circular plate, ductile deformations, theoretical analysis, large deformations

### NOMENCLATURE

$a$	Radius of rigid striker	$N$	Membrane force (per unit length)
$m$	Bending resistance factor at supports	$N_o$	$\sigma_o H$ . Full plastic collapse force of a solid cross-section (per unit length)
$w$	Transverse displacement	$N_r, N_\theta$	Radial and circumferential membrane forces (per unit length), respectively
$E$	Young's modulus of elasticity	$Q_r$	Transverse shear force (per unit length)
$E_r$	Energy ratio	$R$	Plate radius
$G$	Striker mass	$T$	Duration of response
$H$	Plate thickness	$V_o$	Impact velocity
$2L$	Length of a square plate	$W, W_f$	Maximum and permanent transverse displacements, respectively
$M$	Bending moment (per unit length)	$\gamma$	Mass ratio
$M_o$	$\sigma_o H^2/4$ . Full plastic collapse moment of a solid cross-section of a plate (per unit length)	$\epsilon, \dot{\epsilon}$	Strain and strain rate, respectively
$M_r, M_\theta$	Radial and circumferential bending moments (per unit length), respectively	$\kappa_r, \kappa_\theta$	Radial and circumferential changes of curvature, respectively

Received 24 October 2002

\* Dedicated to Professor Narinder K Gupta on his 60<sup>th</sup> birthday

- $\lambda$  Dimensionless initial kinetic energy [Eqns (4) and (12)]
- $\mu$  Mass per unit mid-plane area of plate
- $\rho$  Radius ratio
- $\sigma_0$  Yield strength of plate material
- $\Omega$  Dimensionless initial kinetic energy [Eqn (13)]
- (\*)  $\partial(\ )/\partial t$ ,  $t$  is time.

## 1. INTRODUCTION

Many articles have been published over the years using the rigid-plastic methods of analysis to obtain the dynamic inelastic response of structures<sup>1-7</sup>, but current problems in this field are now often solved using numerical finite-element schemes. However, designers sometimes require approximate methods of analysis, particularly for preliminary design purposes while comparing competing designs before reaching a final decision. Rigid-plastic methods of analysis have been successful in predicting the behaviour of ductile structures subjected to large dynamic loads, mainly because of their reasonable accuracy and comparative simplicity, even when retaining the influence of finite-deformations<sup>8,9</sup>. Moreover, the predictions of these methods are often adequate for final designs when bearing in mind the paucity of information usually available on the dynamic material properties and the characteristics of impact loading.

An approximate theoretical method of analysis was developed by Jones<sup>8,10,11</sup>, *et al.* for the response of beams, plates and shells when subjected to dynamic transverse loads which produce large inelastic strains and permanent deformations. This procedure idealises the structural material as rigid, perfectly plastic and retains the influence of large transverse deflections. The method has been used by a number of authors largely to obtain the structural response for dynamic pressure pulses and for impulsive loadings, and good agreement has been obtained with experimental work conducted on ductile metal beams, plates, and shells loaded impulsively.

The approximate method of analysis<sup>8,10,11</sup> usually can also be used to predict the structural response due to impact loadings. It has predicted relatively

simple expressions for the permanent displacements of beams struck by large masses<sup>12</sup> which agree reasonably well with the experimental results<sup>13</sup>. However, except John<sup>14</sup>, *et al.* no author appears to have used the approximate method to study the impact loading of plates. The analysis by Jones<sup>14</sup>, *et al.* examines the response of a fully clamped circular plate when struck normally by a blunt-ended cylindrical mass, which produces transverse shear sliding in the plate around the periphery of the striker as well as bending deformations and membrane effects within the plate.

Relatively low velocity impacts of plates is a common loading which must be considered in safety calculations, hazard assessments, and safety cases in many industries. The author aims to illustrate the use of the method<sup>8</sup> to study the impact behaviour of circular and square plates and to compare the predictions with the experimental results.

## 2. MASS IMPACT LOADING OF A CIRCULAR PLATE

The theoretical procedure developed<sup>8</sup> and outlined<sup>9</sup> by Norman Jones<sup>14</sup>, was used to examine the response of a rigid, perfectly plastic circular plate of thickness,  $H$ , fully clamped around a circular boundary of radius,  $R$ , and struck normally at the centre by a rigid blunt-ended cylindrical striker of radius,  $a$ , and mass,  $G$ , travelling with an initial velocity,  $V_0$ , as shown in Fig. 1(a). The analysis thus obtained by Jones<sup>14</sup>, *et al.* used the results\* (in terms of equations) in the already reported literature<sup>9</sup> with additional terms related to the influences of the impact mass  $G$  and the transverse shear forces, or

$$\begin{aligned}
 -G\dot{W}\dot{W} - \int_A \mu \dot{w}\dot{w} dA = & \\
 \int_A \{ (M_r + wN_r) \dot{\kappa}_r + (M_\theta + wN_\theta) \dot{\kappa}_\theta \} dA & \\
 + \sum_{m=1}^n \int_{C_m} (M_r + wN_r) (\partial \dot{w} / \partial r)_m dC_m & \\
 + \sum_{u=1}^v \int_{C_u} Q_r(\dot{w})_u dC_u & \quad (1)
 \end{aligned}$$

\* The analysis in Ref (14) used equation 7.103 from Ref (9)

The terms on the left hand side of Eqn (1) are the work rate due to the inertia forces, where  $A$  is the surface area of a plate and  $\mu$  is the mass per unit area. The first term on the right hand side is the energy dissipated in the continuous axisymmetric deformation fields. The second term gives the energy dissipated in  $n$  axisymmetric plastic bending hinges, each having an angular velocity  $(\partial w/\partial r)_m$  across a hinge of length  $C_m$ . The final term is the plastic energy absorption in  $v$  axisymmetric transverse shear hinges, each having a velocity discontinuity  $(\dot{w})_u$  and a length  $C_u$ . Equation (1) ensures that the external work rate equals the internal energy dissipation (Fig. 1).

The dynamic response for the circular plate studied<sup>14</sup> was split into two phases of motion. It can be shown that transverse shear effects are important only during the early phase of motion<sup>9,15</sup>, while membrane forces can dominate subsequent motion. Thus, Eqn (1) without the finite-deflection terms (i.e., membrane forces neglected) controlled the behaviour during the first phase of motion, while Eqn (1) without the transverse shear deformation term governed the behaviour of the final phase of motion.

Equation (1), without the transverse shear term<sup>14</sup>, is used here to illustrate the procedure for obtaining the response of the circular plate impact problem<sup>14</sup>, which is also shown in Fig. 1(a). If the kinematically

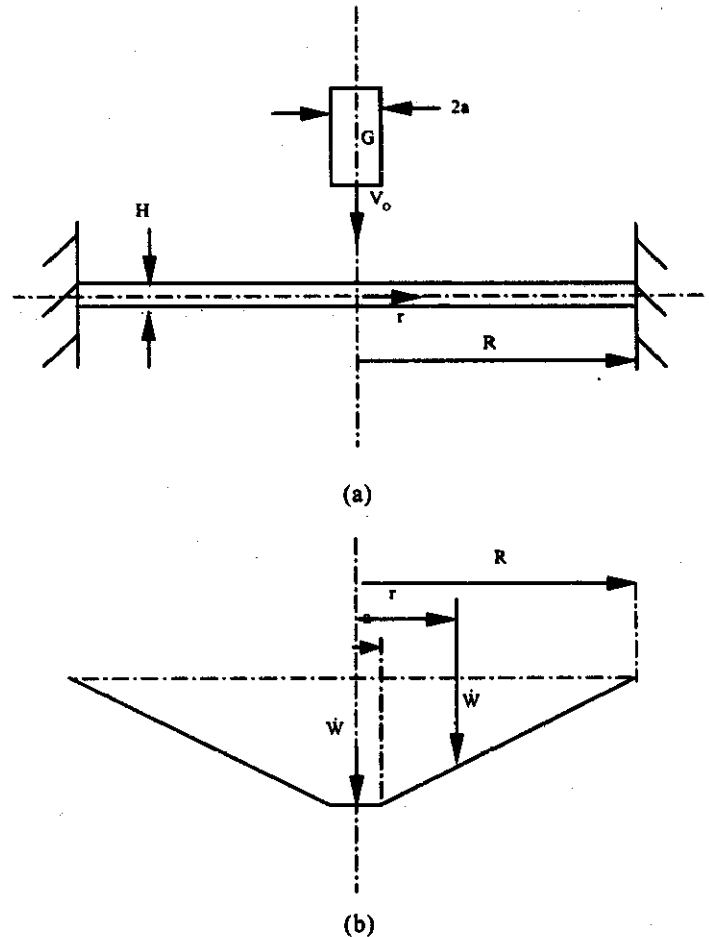


Figure 1. (a) Rigid cylindrical mass  $G$  striking a fully clamped circular plate and (b) axisymmetric transverse velocity profile at time  $t$  for the circular plate in Fig. 1(a).

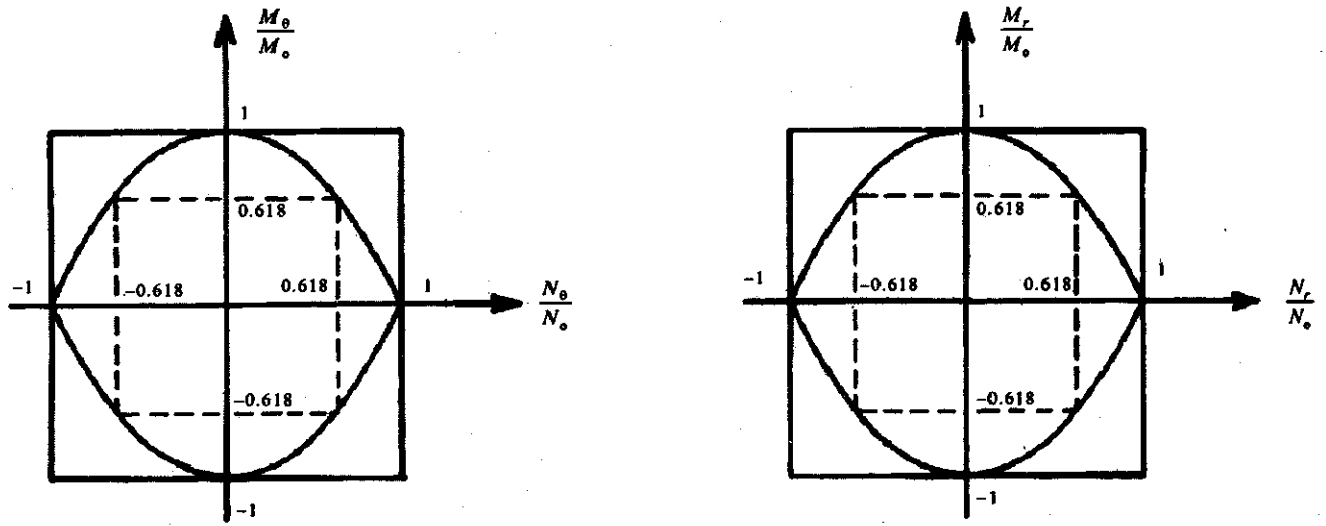


Figure 2. Uncoupled square, or limited interaction, yield condition for the circular plate in Fig. 1

admissible transverse velocity field in Fig. 1(b) governs the response together with the uncoupled square, or limited interaction, yield condition in Fig. 2 and the normality requirements of plasticity, then Eqn (1) reduces to

$$\dot{W} + g^2 W = f \tag{2}$$

where  $f$  and  $g$  are defined\*\* by Eqns[14(a)-14(c)] reported in an earlier paper<sup>14</sup>. The initial velocity at the plate centre,  $\dot{W}_0$  is obtained from the conservation of linear momentum, or

$$\dot{W}_0/V_0 = \{1 + (1 + \rho + \rho^2) / 3\gamma\}^{-1} \tag{3a}$$

where

$$\gamma = G/\mu\pi R^2 \text{ and } \rho = a/R \tag{3b}$$

Now, the solution of Eqn (2) with the initial conditions given by Eqn (3), and  $W_0 = 0$ , predicts the maximum permanent transverse displacement

$$\frac{W_f}{H} = \frac{1}{(1 + \rho)} \left[ \left\{ 1 + \frac{3\gamma^2 \lambda (1 - \rho^2) (6\gamma + 1 + 2\rho + 3\rho^2)}{8(3\gamma + 1 + \rho + \rho^2)^2} \right\}^{1/2} - 1 \right]$$

when motion ceases at  $t = T$

where

$$\lambda = \mu V_0^2 R^2 / M_0 H \tag{4}$$

Equation (4) with  $\rho \ll 1$ , reduces to

$$W_f/H = \{1 + (3\gamma^2 \lambda / 8) (6\gamma + 1) (3\gamma + 1)^{-2}\}^{1/2} - 1 \tag{5}$$

and if  $\rho \ll 1$  and  $\gamma \gg 1$

$$\text{then } W_f/H = \{1 + \gamma \lambda / 4\}^{1/2} - 1 \tag{6}$$

The duration of motion when  $W_f$  given by Eqn(4) is reached, (i.e.,  $\dot{W} = 0$ ), is given by

$$\tan(gT) = (1 + \rho) (V_0 / gH) \{1 + (1 + \rho + \rho^2) / 3\gamma\}^{-1} \tag{7}$$

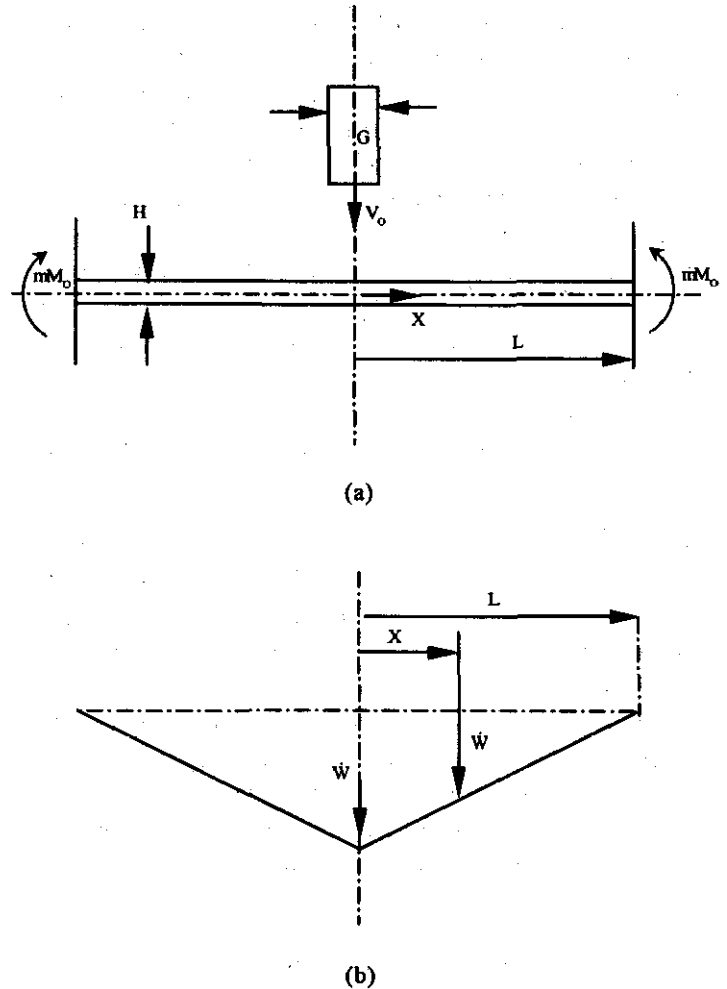


Figure 3. (a) Rigid mass  $G$  striking a square plate having a moment resistance ( $mM_0$ ) around the outer supports ( $m = 0$  and  $m = 1$  give simply supported and fully clamped cases, respectively) and (b) side view of pyramidal-shaped transverse velocity field at time  $t$  for the square plate in Fig. 3(a).

### 3. MASS IMPACT LOADING OF SQUARE PLATE

The general theoretical procedure<sup>8</sup>, which was used to study a circular plate in Section 2, can also be used to obtain the response of a square plate struck by a mass  $G$ , as shown in Fig. 3. In this case, Eqn (1)<sup>\*\*\*</sup> without transverse shear effects takes the simplified form

$$-G\ddot{W}\dot{W} - \int_A \mu \dot{w} \dot{w} dA = \sum_{m=1}^r \int_{\ell_m} (M + Nw) \dot{\theta}_m \ell_m \tag{8}$$

\*\* Note a misprint in Ref(14): the negative sign should be positive in the denominator of equation 14(b) in Ref (14)  
 \*\*\* see also Equation 7.4.2 and 7.4.5 of Ref(9).

for an initially flat, rigid perfectly plastic plate which deforms with a number of rigid regions separated by  $r$  stationary straight line plastic hinges, each of length  $l_m$ .  $\dot{\theta}_m$  is the relative angular velocity across a straight line hinge,  $w$  is the transverse displacement along a line hinge, and  $N$  and  $M$  are the membrane force and bending moment, respectively which act on a plane which passes through a hinge and is transverse to the mid-surface of a plate.

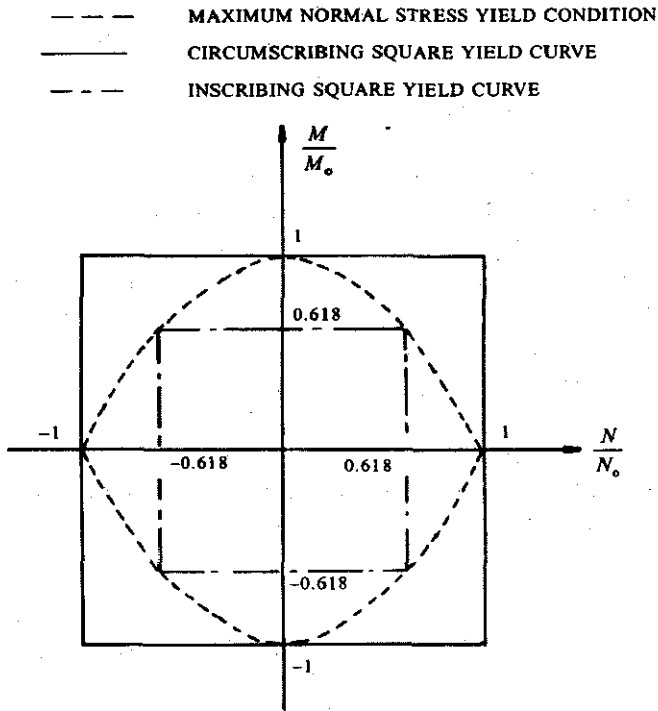


Figure 4. Yield conditions along the plastic hinge lines in the square plate in Fig. 3(a).

Now consider a square plate,  $2L \times 2L$ , which is supported around an outer square boundary having a bending resistance  $mM_0$ , where  $m = 0$  and  $m = 1$  for the simply supported and fully clamped cases, respectively. It is assumed that the mass strikes the centre of a square plate, has a negligible cross-section when compared with the plate dimension,  $L$ , and produces a response characterised by the transverse velocity profile in Fig. 3(b).

Equation (8) for the impact problem in Fig. 3(a) when using the transverse velocity field in Fig. 3(b) and the square yield condition in Fig. 4, yields the governing differential equation:

$$\ddot{W} + \alpha^2 W = -\alpha^2 H(1+m)/2 \quad (9)$$

where

$$\alpha^2 = (24M_0/\mu L^2 H) (6\gamma + 1)^{-1}$$

and

$$\gamma = G/4\mu L^2$$

The peak value of the initial velocity,  $\dot{W}_0$ , for the velocity profile in Fig. 3(b), is obtained from the conservation of linear momentum, or

$$\dot{W}_0/V_0 = (1 + 1/3\gamma)^{-1} \quad (10)$$

Now, solving Eqn (9) and introducing the initial conditions  $W_0 = 0$  and Eqn (10) for  $\dot{W}_0$  to eliminate the constants of integration, yields an expression for the time-dependent deflection of the plate. The motion of the plate ceases when  $\dot{W}_0 = 0$  at  $t = T$ , where

$$\tan(\alpha T) = (2V_0/\alpha H) (1+m)^{-1} \quad (11)$$

and the associated maximum permanent transverse displacement at the plate centre is

$$W_f/H = (1+m) \quad (12)$$

$$\left[ \left\{ 1 + 3\lambda\gamma^2 (6\gamma+1)(3\gamma+1)^{-2} (1+m)^{-2} / 2 \right\}^{1/2} - 1 \right] / 2$$

where

$$\lambda = \mu V_0^2 L^2 / M_0 H$$

Equation (12) with  $\gamma \gg 1$  for a large impact mass relative to the plate mass gives:

$$W_f/H = (1+m) \left[ \left\{ 1 + \lambda\gamma (1+m)^{-2} \right\}^{1/2} - 1 \right] / 2$$

or

$$W_f/H = (1+m) \left\{ (1+\Omega)^{1/2} - 1 \right\} / 2 \quad (13)$$

where

$$\Omega = GV_0^2 / \{(1+m)^2 \sigma_0 H^3\}$$

It should be noted that if  $\Omega \gg 1$  and  $\Omega^{1/2} \gg 1$  for very large impact loadings producing large permanent transverse displacements  $W_f / H \gg 1$ , then

$$W_f / H \cong (GV_0^2 / 4\sigma_0 H^3)^{1/2} \tag{14}$$

which is independent of the boundary resistance factor,  $m$ , because of the dominance of membrane effects.

#### 4. DISCUSSION

##### 4.1 General Remarks

The theoretical procedure developed<sup>8-11</sup>, and applied in Sections 2 and 3 for the impact loadings of circular and square plates, assumes that the material is rigid-perfectly plastic. In other words, the influence of material elasticity is ignored for impact loadings producing relatively large plastic strains. This assumption is reasonable when the initial kinetic energy is much larger than the maximum strain energy that can be absorbed by a structure in a wholly elastic manner. A conservative ratio between these two energies gives an energy ratio<sup>9</sup>, or

$$E_f = \gamma \lambda (E/\sigma_0) (H/2R)^2 \tag{15a}$$

and

$$E_f = \Omega (1+m)^2 (E/\sigma_0) (H/2L)^2 \tag{15b}$$

for the impact loaded plates in Figs 1(a) and 3(a), respectively.

The theoretical analyses use the transverse velocity fields in Figs 1(b) and 3(b) which disregard any possible transient phase of motion. This simplification was studied<sup>16</sup> for a rigid, perfectly plastic beam struck on the span by a rigid mass. It was found that such an analysis for beams with striker mass-to-beam mass ratios larger than 16.58 gave errors of less than 2 per cent when compared with an

exact solution. A mass ratio larger than 8.25 leads to differences which are less than 4 per cent. Similar comparisons have not been reported for circular and square plates, but it might be anticipated that  $\gamma$ , which is given by Eqns (3) and (9), would be related to similar differences.

It can be shown that Eqns (1) and (8) for the specific case of impulsive velocity loadings and infinitesimal displacements reduce to the form of Martin's theorem<sup>15,17</sup>, so that such an analysis predicts a rigorous upper bound value for the maximum permanent displacements of rigid, perfect plastic continua and structures.

The theoretical analyses in Sections 2 and 3 employ the simplified yield conditions in Figs 2 and 4 which circumscribe the corresponding exact yield criteria. It is indicated that similar yield conditions, but having all dimensions 0.618 times as large would inscribe the associated exact one. Theoretical predictions for circumscribing and inscribing yield criteria are shown in Figs 5 to 7. It might be reasonable to assume that these predictions offer upper and lower bounds on the exact solution, although no theorems proving this supposition exist<sup>9</sup>.

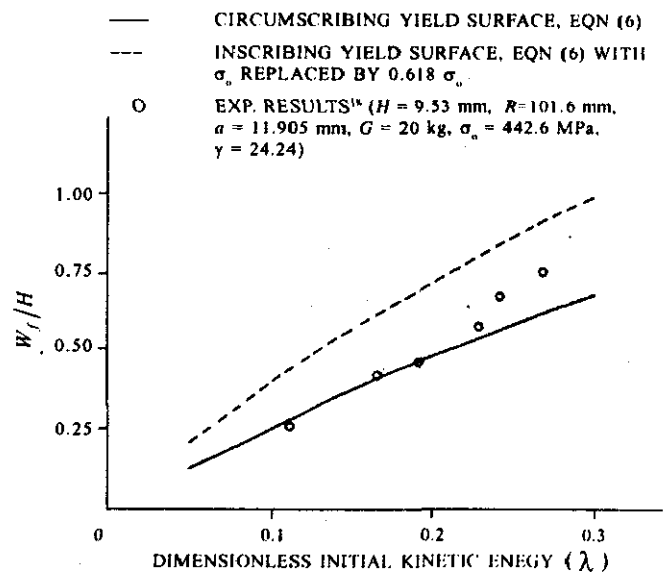


Figure 5. Comparison of the theoretical predictions of Eqn (6) with experimental results on fully clamped aluminium alloy circular plates struck by masses at the centre.

The method of analysis could be used to obtain theoretical solutions for an exact yield condition<sup>8,9</sup> for the blast loading of beams and rectangular plates. It transpires that these predictions are bounded by simpler theoretical solutions using approximate yield criteria which circumscribe and inscribe the exact yield surface.

#### 4.2 Circular Plates

The theoretical predictions of Eqn (6), and the predictions of Eqn (6) with  $\sigma_0$  replaced by  $0.618\sigma_0$  for an inscribing yield condition, essentially bound the experimental values in Fig. 5 for the maximum permanent transverse displacements of the impact loaded aluminium alloy plates<sup>18</sup>. However, the energy ratios  $E_r$  according to Eqn (15) range from about 1 to 3 for the experimental values in Fig. 5. These are small ratios, although  $E_r$  is defined very conservatively<sup>9</sup> because local plastic deformations would occur at much smaller values of the elastic strain energy than the crude estimate which is used in the denominator of Eqn (15). Rigid, perfectly plastic analyses have given acceptable predictions for beams with energy ratios<sup>19</sup> as small as 3, but the comparisons in Fig. 5 suggest that reasonable accuracy can be obtained for even smaller energy ratios for plates.

The theoretical predictions of Eqn (5), and of Eqn (5) with  $0.618\sigma_0$  replacing  $\sigma_0$ , bound the experimental results in Fig. 6 for the maximum permanent transverse displacements recorded by Tian and Jiang<sup>20</sup> on fully clamped circular plates struck by a mass at the centre. These test results were designed to explore the phenomenon of scaling and were obtained on geometrically similar plates having different thicknesses over a scale range of four. The energy ratios,  $E_r$ , for the experimental data in Fig. 6, are between about 10 to 15 according to Eqn (15). However, the mass ratio for these tests is  $\gamma = 1.33$  according to Eqn [3(b)], which for the mass impact behaviour of a beam<sup>16</sup>, would lead to an error of about 10 per cent when compared with an exact solution. Unfortunately, no similar studies have been reported on plates, so that the error is not known for the impact behaviour of a plate with  $\gamma = 1.33$ .

The experimental data<sup>20</sup>, which is plotted in Fig. 6, was obtained using YB 231-70 20g steel plate. This steel has low material strain rate sensitive properties since the flow stress at a strain rate of 17/s increases only by 5 per cent when compared with the static flow stress. This should be compared with an average strain rate of about 7/s for those test specimens in Fig. 6 with  $W_f/H \approx 3$ , according to the equation given in the footnote on p.376 of Ref (9). Thus, material strain rate effects are not expected to exercise a significant influence on the response.

#### 4.3 Square Plates

Some recent experimental values obtained in the Impact Research Laboratory at the University of Liverpool are presented in Fig. 7 for the maximum permanent transverse displacements of fully clamped square steel plates struck by a mass at the centre. It is evident that the theoretical analysis given by Eqn (13), and by Eqn (13) with  $\sigma_0$  replaced by  $0.618\sigma_0$ , bound all of the experimental data. The ratios  $\gamma$  and  $E_r$  are much larger than the one for all of the test results in Fig. 7. Unfortunately, the strain rate sensitive behaviour of the material used for all of the square plates in Fig. 7 has not been obtained and, moreover, no experimental data appears

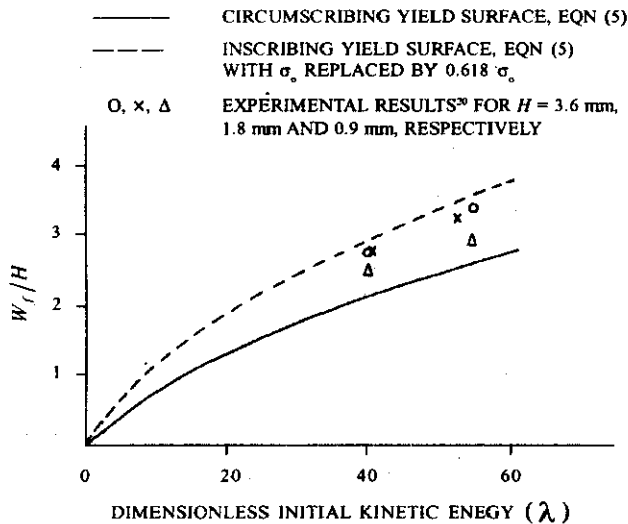
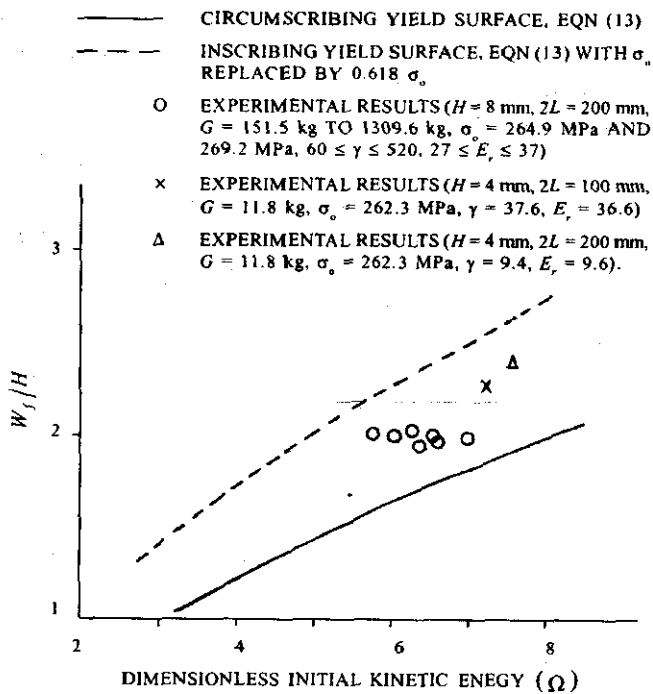


Figure 6. Comparison of the theoretical predictions of Eqn (5) with experimental results on fully clamped steel circular plates struck by a mass at the centre.



**Figure 7. Comparison of the theoretical predictions of Eqn (13) with experimental results on fully clamped steel square plates struck by a mass at the centre.**

to have been published for square aluminium alloy plates struck by large masses.

#### 4.4 Final Comments

The agreement between the theoretical predictions of Section 2 on circular plates and the experimental results in Figs 5 and 6 is very encouraging, particularly because there is no uncertainty on the influence of material strain rate sensitivity. The aluminium alloy plates in Fig. 5 are made from a strain rate insensitive material, while, this phenomenon has an essentially negligible influence on the behaviour of the grade of the steel plates reported in Fig. 6. Figure 7 shows similar agreement between the theoretical predictions and experimental results for square plates despite being made of steel: Albeit with unknown material strain rate sensitivity characteristics.

Now, it is estimated<sup>9</sup> that the average strain rate is  $\dot{\epsilon} \cong v_0 W_f / (3\sqrt{2}L^2)$  in a square plate which predicts  $0.8 < \dot{\epsilon} < 2.3/s$ , approximately, for the plates designated as O in Fig. 7. Similarly, strain rates of 1.7/s and 6.5/s are estimated for the experimental

results identified as Δ and X, respectively. These strain rates are small, but not negligible. It is well known that the strain rate sensitivity of steels decrease with an increase in strain [eg, 19]. Thus, the influence of this phenomenon on the plates in Fig. 7 should be less important than that associated with the usual strain rate sensitive coefficients evaluated for the yield stress. Clearly, more information is required on the strain rate sensitive characteristics of the materials used for the square plates in Fig. 7.

The kinematically admissible transverse velocity profiles in Figs 1(b) and 3(b) are adequate for the range of parameters studied in Figures 5–7. However, it might be necessary to modify these transverse velocity fields for other cases, such as conical, hemispherical or other shaped impactors, or for impacts at non-central locations and for rectangular plates.

If the impact energies are sufficiently large, then a plate might crack. The threshold conditions for cracking have not been examined here, since these have been explored by many authors, including some recent studies on the impact failure of beams<sup>22</sup> and circular plates<sup>23</sup>. Perforation of a plate could occur for even higher impact velocities.<sup>14,18,24-28</sup>

#### 5. CONCLUSIONS

The response of circular and square plates, which are struck by a rigid mass at the plate centre, are studied using a simplified analysis which assumes that the plates are made from a rigid, perfectly plastic material. This theoretical method retains the influence of finite transverse displacements and could be used to study the behaviour of plates having any shape, a variety of boundary conditions, and a wide range of external dynamic loadings. Theoretical solutions using this method have already been published for the impact and blast loadings of beams, and the blast loading of plates and shells. Reasonable agreement between the theoretical predictions and experimental test results on ductile metal structures has been observed in the previous studies as well as in the present study. The main advantage of the theoretical predictions lies in their simplicity and value for preliminary design studies.

The theoretical analyses and test specimens in the experimental programmes have large ductile deformations without any failure. However, the particular impact loading cases examined here are important potential test arrangements for obtaining the threshold conditions for failure (i.e., cracking). The test arrangement can be carefully controlled and the drop height of the striker raised until cracking just occurs in a virgin plate. Such tests are valuable for seeking the appropriate criterion which controls failure in collaboration with robust numerical finite-element codes.

### ACKNOWLEDGEMENTS

The author wishes to express his appreciation to Dr R.S. Birch, Mr Y.K. Ho, Mr S. Kolovos and Mr S.E. Song for their assistance with experimental results in Fig. 7, and to Mrs M. White and Mrs I. Arnot for typing the manuscript and tracing the figures.

### REFERENCES

1. Gupta, N.K. & Sengupta, S.(Eds). Large deformations, Proceedings of Symposium in Memory of Professor B. Karunes. South Asian Publishers Pvt, New Delhi, 1982.
2. Gupta, N.K. (Ed). Plasticity and impact mechanics. New Delhi, Wiley Eastern Ltd., 1993.
3. Gupta, N.K. (Ed). Plasticity and impact mechanics. New Delhi: New Age International (P) Ltd. Publishers, 1997.
4. Johnson, W. & Reid, S.R. Metallic energy dissipating systems. *Appl. Mech. Rev.*, 1978, **31**, 277-88.
5. Johnson, W & Reid, S.R. Metallic energy dissipative system—an update. *Appl. Mech. Rev.*, **39**, 315-19.
6. Jones, N. Recent studies on the dynamic plastic behaviour of structures. *Appl. Mech. Rev.*, 1989, **42**(4): 95-115.
7. Jones, N. Recent studies on the dynamic plastic behaviour of structures—an update. *App. Mech. Rev.*, 1996, **49**(10), 112-17.
8. Jones, N. A theoretical study of the dynamic plastic behaviour of beams and plates with finite-deflections. *Int. J. Solids Struct.*, 1971, **7**, 1007-29.
9. Jones, N. Structural impact. Cambridge University Press, 1989. Paperback edition, 1997. Chinese edition translated by Ping Jiang and Lili Wang, Sichuan Education Press, Chengdu, 1994.
10. Walters, R.M. & Jones, N. An approximate theoretical study of the dynamic plastic behaviour of shells. *Int. J. Nonlinear Mech.*, 1972, **7**(3), 255-73.
11. Jones, N. & Walters, R.M. A comparison of theory and experiments on the dynamic plastic behaviour of shells. *Archives Appl. Mech.*, (Olszak Anniversary Volume), 1972, **24**(5-6), 701-14.
12. Liu, J. & Jones, N. Dynamic response of a rigid plastic clamped beam struck by a mass at any point on the span. *Int. J. Solids Struct.*, 1988, **24**(3), 251-70.
13. Liu, J and Jones, N. Experimental investigation of clamped beams struck transversely by a mass. *Int. J. Impact Engg.*, 1987, **6**(4), 303-35.
14. Jones, N.; Kim, S.B. & Li, Q.M. Response and failure analysis of ductile circular plates struck by a mass. (*Trans. ASME*), *J. Pressure Vessel Tech.*, 1997, **119**(3), 332-42.
15. Jones, N. Bounds on the dynamic plastic behaviour of structures including transverse shear effects. *Int. J. Impact Engg.*, 1985, **3**(4), 273-91.
16. Jones, N. Quasi-static analysis of structural impact damage. *J. Constructional Steel Res.*, 1995, **33**(3), 151-77.
17. Martin, J.B. Impulsive loading theorems for rigid-plastic continua. (Proceedings of the ASCE). *J. Engg. Mech. Div.*, 1964, **90**(EM5), 27-42.

18. Wen, H.M. & Jones, N. Experimental investigation into the dynamic plastic response and perforation of a clamped circular plate struck transversely by a mass. *Proceedings I.Mech.E.* 1994, **208**(Part C2), 113-37.
19. Bodner, S. R. & Symonds, P. S. Experimental and theoretical investigation of the plastic deformation of cantilever beams subjected to impulsive loading. *J. App. Mech.*, 1962, **29**, 719-28.
20. Tian, C. & Jiang, P. Experimental investigation of the scaling laws for circular plates struck by projectiles. *In Proceedings of the IUTAM Symposium on Impact Dynamics*, edited by Z. Zheng and Q. Tan. Peking University Press, 1994. pp. 440-45.
21. Jones, N. Some comments on the modelling of material properties for dynamic structural plasticity. *International Conference on the Mechanical Properties of Materials at High Rates of Strain*, edited by J. Harding. Institute of Physics-Conference Series 1989, Oxford. **102**: pp. 435-45.
22. Yu, J. & Jones, N. Numerical simulation of impact loaded steel beams and the failure criteria. *Int. J. Solids Struct.*, 1997, **34**(30), 3977-004.
23. Jones, C. & Jones, N. Inelastic failure of fully clamped beams and circular plates under impact loading. *Proceedings I. Mech. E.* 2002; 216(Part C). *J. Mech. Engg. Sci.*
24. Gupta, N. K. & Madhu, V. Normal and oblique impact of a kinetic energy projectile on mild steel plates. *Int. J. Impact Engg.*, 1992, **12**(3), 333-43.
25. Gupta, N.K.; Ansari, R. & Gupta, S.K. Normal impact of ogive-nosed projectiles on thin plates. *Int. J. Impact Engg.*, 2001, **25**(7), 641-60.
26. Borvik, T.; Langseth, M.; Hopperstad, O.S. & Malo, K.A. Perforation of 12 mm thick steel plates by 20 mm diameter projectiles with flat, hemispherical and conical noses. Part 1: Experimental study. *Int. J. Impact Engg.*, 2002, **27**(1), 19-35.
27. Corbett, G.G.; Reid, S.R. & Johnson, W. Impact loading of plates and shells by free-flying projectiles: A review. *Int. J. Impact Engg.*, 1996, **18**(2), 141-30.
28. Goldsmith, W. Non-ideal projectile impact on targets. *Int. J. Impact Engg.*, 1999, **22**(2-3), 95-395.

### Contributor



**Professor Norman Jones** is Director of the Impact Research Centre, Dept of Engineering (Mech Engg), The University of Liverpool, UK. He has conducted theoretical, numerical and experimental studies over the past 35 years into the dynamic inelastic behaviour of structures and systems. His more recent studies have focused on the dynamic inelastic failure of structures subjected to impact loads to seek the appropriate failure criterion for use in design and in computer codes, the formation of shear localisations in structural elements and the influence of hydrostatic stress on failure. Experimental investigations have been conducted for hazard assessments and safety calculations throughout industry when the impact speeds are much smaller than ordnance levels and the methods of analysis must cope with fundamental differences in the response. The behaviour of sandwich panels and laminates under static and dynamic loads and thermoplastic-based fibre-metal laminates have also been studied. He is Editor-in-Chief of the *International Journal of Impact Engineering*, Associate Editor of *Applied Mechanics Reviews* (U.S.) and is on the editorial boards of several other international journals. He has published more than 200 research papers and has authored a book. He has won two prizes from the Institution of Mechanical Engineers, one from the Royal Institution of Naval Architects, a *Distinguished Scientist Award* from the Wessex Institute of Technology. He was elected to the Royal Academy of Engineering in 1998.